

Electron-conformational interactions and the low-temperature Mössbauer line broadening in $\text{Fe}_3[\text{Co}(\text{CN})_6]_2 \cdot 12\text{H}_2\text{O}$

Alexandre I. Rykov¹, Kiyoshi Nomura², Junhu Wang^{1,*}

¹ Mössbauer Effect Data Center, Dalian Institute of Chemical Physics, Chinese Academy of Sciences, 457 Zhongshan Road, Dalian 116023, China

² Photocatalysis International Research Center, Tokyo University of Science, Yamazaki 2641, Noda, Chiba Pref., 278-8510, Japan

*corresponding author e-mail address: wangjh@dicp.ac.cn

ABSTRACT

The interactions between valence electrons of a 3d metal ion and the conformations of surrounding ligands play an important role in Prussian blue analogues (PBA). In the PBA $\text{Fe}_3[\text{Co}(\text{CN})_6]_2 \cdot 12\text{H}_2\text{O}$, the high-spin Fe^{2+} is surrounded by the ligands of two sorts. One sort is negatively charged CN^- (at its N-end) and another one is neutral (H_2O), but allowing by virtue of proton conductivity the charged states OH^- and H_3O^+ . The electron-conformational interactions (ECI) yield a number of ground states for the Fe^{2+} ion. The existence of a variety of conformations ensues from the cubic structure with random occupation of the ligand site by the CN^- and H_2O species. A crystal field-splitting schema is distinct for each conformation. In particular, the orbital doublet (OD) is the ground state for the trans-conformation of two H_2O ligands. The orbital singlet (OS) state becomes lowest for the cis-conformation. In Mössbauer spectra (MS), the quadrupole splitting (QS) ΔE_Q correlates with the strength of crystal field and is typically of ca. 1 and 2 mm/s for the OD and OS, respectively, at 300 K, increasing at 77 K to ca. 2 and 3 mm/s (viz, in $\text{Fe}[\text{Co}(\text{CN})_6]_{2/3}$). The concept of ECI is the plausible approach explaining the motional narrowing observed in MS. As temperature increases from 77 K to 300 K the linewidths of the quadrupole subspectrum associated with the OD ground state decreases most dramatically. We explain this by the motional averaging within the ΔE_Q values characteristic of each conformation. Such a motion is strongly correlated among the neighbouring cells, therefore, it can be viewed as the collective motion of the so-called conformon quasiparticles.

Keywords: Prussian Blue, hexacyanocobaltate, Mössbauer spectroscopy, motional narrowing.

1. INTRODUCTION

Prussian blue analogues (PBA) include a broad family of hydrated double metal cyanide frameworks $\text{M}_3[\text{M}'(\text{CN})_6]_2 \cdot 12\text{H}_2\text{O}$ with the coordinated ions of metals M and M' in octahedra MN_6 and $\text{M}'\text{C}_6$ connected by their vertices via the CN bridges [1-3]. Recently, several PBA family members enclosing the 3d metal ions have excited much interest owing to salient properties related to linkage isomerism, charge transfer and spin-state phase transitions [4-6]. Depending on the structure features, such as 3d ion configurations and valences, ionic size mismatch, hydration degree, etc., the crystalline framework may experience either precipitous or continuous transformations. In particular, the sharp spin-state transition was observed in $\text{CsFe}[\text{Cr}(\text{CN})_6] \cdot \text{H}_2\text{O}$, and the strong crystal field was argued to induce the spin-state transition on the Fe^{2+} ion[5].

However, in the alkali-free hexacyanometallates $\text{Fe}_3[\text{Cr}(\text{CN})_6]_2 \cdot 12\text{H}_2\text{O}$ and $\text{Fe}_3[\text{Co}(\text{CN})_6]_2 \cdot 12\text{H}_2\text{O}$ the spin-state transition was not observed. A weaker crystal field was implied[5]. In this work, we reinvestigate the latter compound, and observe the Mössbauer line broadening between 170 and 250 K. Instead of spin-state crossover we observe the gradual linewidth crossover related to intrinsic ligation disorder among the CN and H_2O in $\text{Fe}_3[\text{Co}(\text{CN})_6]_2 \cdot 12\text{H}_2\text{O}$ rather than to a change in the spin degree of freedom. Vice versa, as temperature increases, we observe strong narrowing of the lines. As the thermal motion becomes sufficient, the crystal field energy landscape flattens out because the local environments of Fe^{2+} on the timescale of the ^{57}Fe probe averages out. There remains an energy barrier between

different conformations, for example, between cis- and trans- $\text{Fe}(\text{CN})_4(\text{H}_2\text{O})_2$, associated with different quadrupole splitting in MS [7]. In contrast, thermal motion averages out the tautomer's energy for the water cluster composed of coordinated water molecules (H_2O)₆ and zeolite waters[8-10]. The tautomeric transitions within the molecular cluster are, to a large extent, similar to conformons[11].

Therefore, we believe that the linewidth contraction can be explained in terms of conformon dynamics. The conformon can be viewed as a composite quasiparticle whose displacement signifies the configurational change in a Fe^{2+} ion and the coupled jump of a water molecule or a proton in a vicinity of the central Fe^{2+} ion. Conformational dynamics turns on when the diffusive motion unfreezes. A quasiparticle coined "conformon" was denoted by Volkenstein [12, 13] as "a cluster of electronic density which is transferred in a biopolymer together with a conformational deformation of the neighboring groups", otherwise, "the displacement of the electronic density in a macromolecule that produces the deformation of the lattice, i.e. the conformational strain[12, 13]."

While the characteristic time of the thermal vibrational excitations are of the order of 10-13 s, the conformational excitations are much slower and characterized typically by $t = 10^{-5}$ to 10^{-9} s. These values are comparable to the lifetime of the excited Mössbauer nucleus ^{57}Fe . Therefore, since the electron-conformational excitations fall into the Mössbauer time window we expect them being detectable in the spectra of ^{57}Fe .

Thus, in this work, our goal was to investigate the detailed temperature dependence of the Mössbauer spectra $\text{Fe}_3[\text{Co}(\text{CN})_6]_2 \cdot 12\text{H}_2\text{O}$ and to understand the role of the

conformational disorder on the Mössbauer spectra and eventually on the motional dynamic phase transition induced thermally in this compound.

2. EXPERIMENTAL SECTION

The PBA compound $\text{Fe}_3[\text{Co}(\text{CN})_6]_2 \cdot 12\text{H}_2\text{O}$ (hereafter called Fe-Co PBA) samples were synthesized with the natural abundance of Mössbauer nuclei (sample 1) and enriched with ^{57}Fe [2]. The sample 1 was precipitated from salts solution, mixing the 0.025 M aqueous solution of $\text{K}_3[\text{Co}(\text{CN})_6]$ with 0.025 M solutions of $\text{FeCl}_2 \cdot 4\text{H}_2\text{O}$. The sample 2 was prepared mixing the 0.025 M aqueous solution of $\text{K}_3[\text{Co}(\text{CN})_6]$ with the solution obtained by heating the powder $^{57}\text{Fe}_2\text{O}_3$ stirred in HCl of corresponding (weak) molarity.

Analytic methods of inductively coupled plasma and x-ray-fluorescent analysis gave the results consistent with the above formula and with site occupancies obtained from Rietveld

analysis. The water content in the samples was estimated by thermogravimetric analysis carried out using a Setaram Setsys 16/18 analyzer measuring the weight loss in the air flow of 25 mL/min with a heating rate of 10 K/min.

X-ray Diffraction (XRD) patterns analysed with Rietveld method confirmed that both 1 and 2 are the single-phase samples.

Mössbauer spectra were measured with a Topologic 500 A spectrometer at the temperatures between 78 K and room temperature. Mössbauer source $^{57}\text{Co}(\text{Rh})$ of approximately 20 mCi was employed. Isomer shift are given in all spectra relative to $\alpha\text{-Fe}$.

3. RESULTS SECTION

In the case of the d6 configuration for the Fe^{2+} ion the Volkenstein's "displacement of electron density" concerns the location of the sixths d-electron only, which is placed either on the doubly degenerate (dxz , dyz) orbital, or on the undegenerate dx_y orbital. The conformation of water molecules surrounding the central Fe^{2+} ion controls the degree of degeneracy (Fig.1). The ground state of the Fe^{2+} ion may turn from orbital singlet (OS) to orbital doublet (OD) and vice versa when the charge state of a ligand changes.

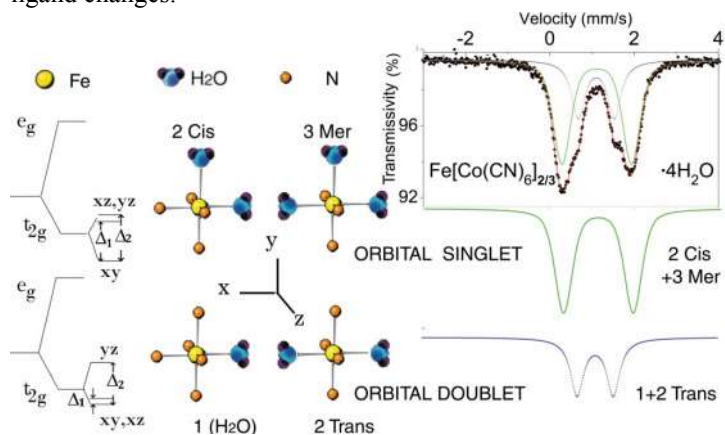


Figure 1. The primary schemes of crystal field splitting (left), the dominant ligand conformations (center), and Mössbauer spectra and main subspectra in 1 (right) assigned to the orbital singlet and orbital doublet ground states stabilized in oblate (meridional and Cis) and prolate (Trans, and unilateral) arrangements of H_2O .

Mössbauer spectra in 1 and 2 are shown in Figures 1 and 2, respectively. It is shown in Fig.1 that the most populated asymmetric conformations of waters (2Cis and 3Mer) give rise to the orbital doublet with larger QS, whereas more symmetric conformations (1 and 2Trans) give rise to the orbital singlet with smaller QS. In previous work [14], more details of the subspectra assignments can be found. Along with other (minority) sites, in total, four doublets were implemented in fitting procedures, three of which belong to Fe^{2+} and one to Fe^{3+} . Only two major doublets are shown for simplicity in Fig.1, and all four doublets are shown

in Fig. 2. In room temperature spectra, the contributions of Fe^{3+} in samples 1 and 2 are 5% and 29%, respectively. The linewidth of the Fe(III)-doublet is roughly temperature-independent, in agreement with the attribution of this minority feature to a separate Fe-O phase [15].

In the linewidths of three Fe^{2+} doublets we observe the step-like anomalies between 200K and 250K. Thin-sample approximation and transmission integral regime were applied in the absorbers of different thickness prepared from samples 1 and 2, respectively. In both regimes, MOSSWINN 4.0 program fitting the spectra [16]. The improved statistical quality of the spectra in sample 2 allowed a detailed study of the high-quality spectra collected in the broad temperature range with the step $\Delta T = 15$ K (Fig. 2).

In the transmission integral regime of the MOSSWINN 4.0 program [17], the lineshapes are approximated by pseudo-Voigtian functions, consisting of Lorentzian and Gaussian parts [18]. The source linewidth was fixed to 0.15 mm/s and the Lorentzian part of each doublet linewidth was fixed to the value of natural linewidth $\Gamma_N = 0.097$ mm/s. The major contributions into each doublet linewidth are produced by the Gaussian term arising from inhomogeneous broadening [19]. From the peak-height spectra analysis and radiation filtering tests the background fraction was derived, $b = 0.1$, which is the fraction of the spectral baseline corresponding to spurious not Mössbauer counts recorded by the detector [20, 21]. The source f -factor at room temperature $f_s = 0.68$ was estimated using an absorber of enriched α -iron foil as described previously [22, 23].

Important parameters extracted from the spectra treatment regime are shown in Figures 3 and 4. The adjustable parameters include 5 global ones (baseline N, background fraction b, source f -factor f_s , source linewidth Γ_s and thickness t). The Lorentzian linewidths Γ_N , as well as b, f_s and Γ_s were fixed in the final run identical for all spectra. The inhomogeneous broadening

associated with $\Gamma(T)$ reflects the Gaussian distribution of quadrupole splitting around the mean $\Delta E_Q(T)$ value.

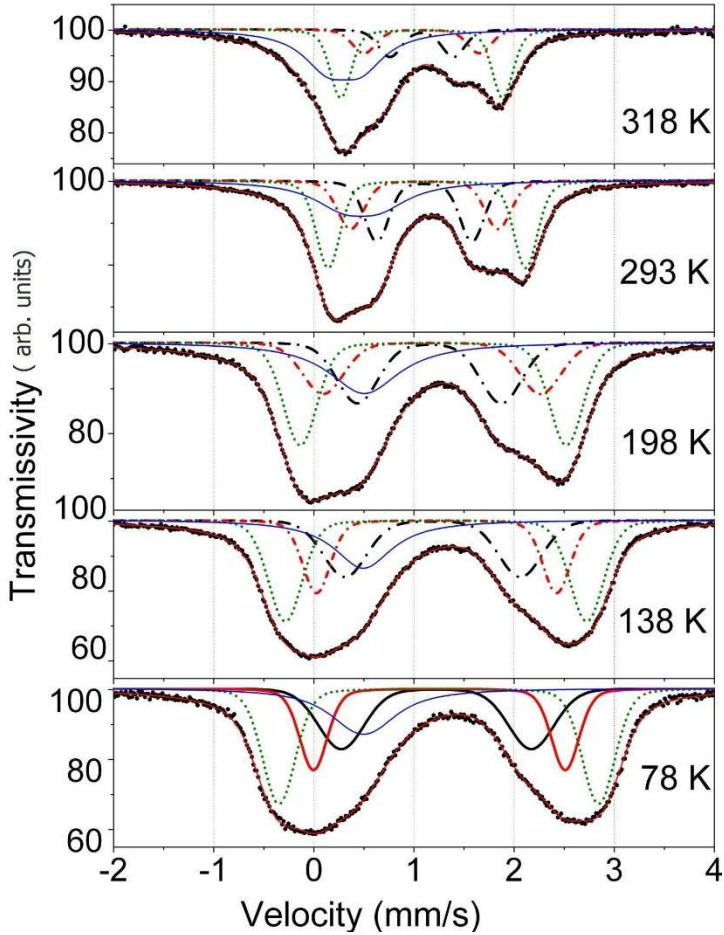


Figure 2. Mössbauer spectra of 2 at 78, 138, 198, 293 and 318 K fitted in transmission integral regime with four quadrupole doublets.

Left panel in Fig. 3 shows the temperature dependence of the dimensionless Mössbauer thickness $t = \sigma_0 \beta n f_{LM}$, where $\sigma_0 = 2.56 \times 10^{-18} \text{ cm}^2$ is the resonant cross-section, β is the enrichment fraction, n is the density of resonant nuclei per cm^2 , and f_{LM} is the Lamb-Mössbauer factor:

$$f_{LM}(T) = \exp\left(-E_R \int_0^\infty \frac{g(E)}{E} \coth\left(-\frac{E}{2k_B T}\right) dE\right) \quad (1)$$

Here the temperature dependence of the Lamb-Mössbauer factor is expressed through the phonon density of states $g(E)$, the phonon energy E , the Boltzmann's constant k_B and temperature T . The recoil energy E_R received by a free atom with mass M is defined by the energy conservation law, $E_R = E_\gamma / 2Mc^2$ ($E_R \approx 0.002 \text{ eV}$ for ^{57}Fe). Here E_γ is the energy of γ -radiation and c is the light velocity. A step-like anomaly observed in the plot of the effective thickness t vs. T signifies some change in the shape of the density of states (DOS). The factor $1/E$ in Eq. (2) enhances the effect of low-energy excitations on the temperature dependence of $f_{LM}(T)$. The long-wave excitations contribute less to low-energy part of DOS $g(E)$ as they freeze out at $T_f \approx 230 \text{ K}$.

The Fe^{3+} area fraction (also plotted in the left panel of Fig.3) contains contributions of high-spin Fe^{3+} in main phase and in external Fe-O phase. The Fe-O impurity phase[14] is unmasked at higher temperature owing to the higher $f_{LM}(T)$ factor. In Fig. 3, the temperature dependence of the fitted effective thickness is the global parameter, involving both contributions, $c(\text{Fe}^{2+})f_{LM}^{2+}(T) + c(\text{Fe}^{3+})f_{LM}^{3+}(T)$.

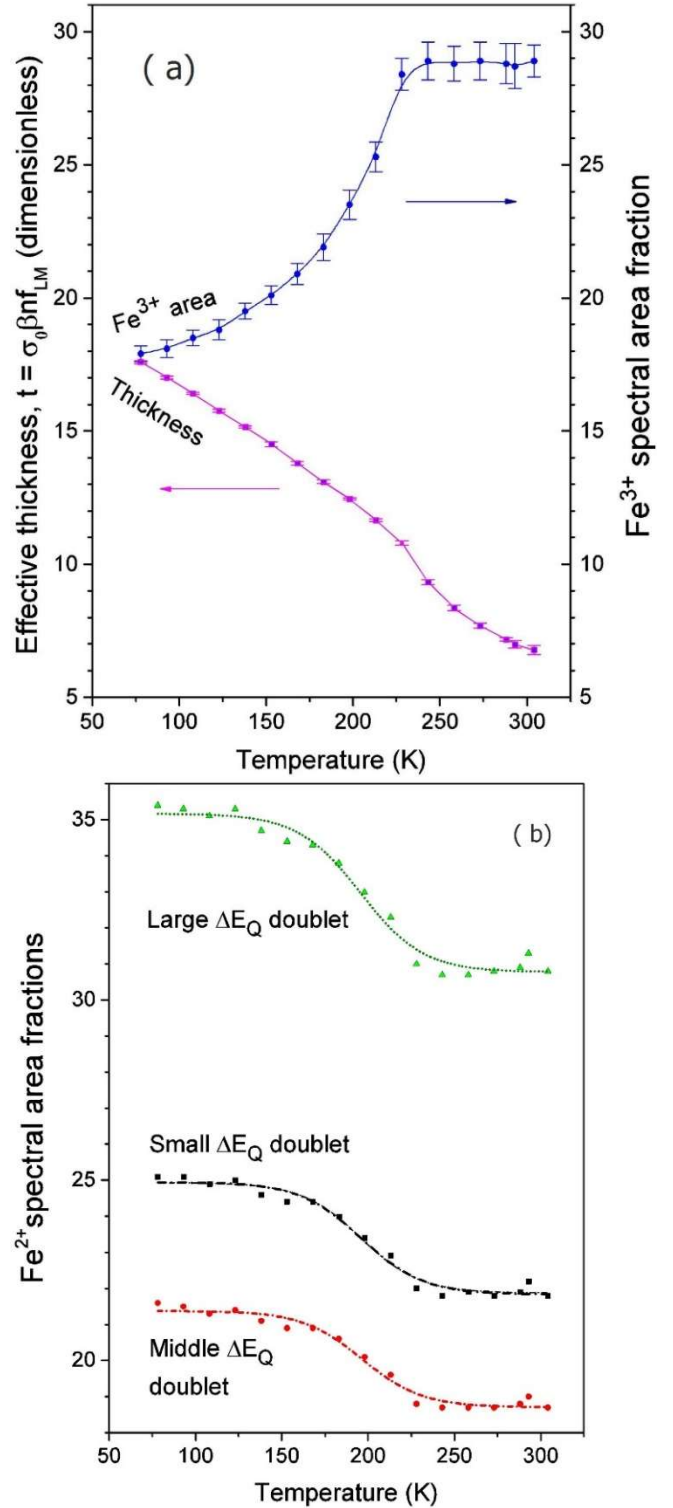


Figure 3. Temperature dependences of the effective Mössbauer thickness and Fe^{3+} subspectrum area fraction (a) and three Fe^{2+} doublets area fractions (b) in 2.

Assuming that the oxide impurity in PBA coined previously [15] “Fe-O phase” is the ferrihydrite we estimate the Debye temperatures (Θ_D) in a partially oxidized PBA of 500K [24] and 200K [25] for the secondary and primary phases, respectively. Because of the difference of Θ_D and δ (isomer shifts) between the Fe^{2+} and Fe^{3+} phases the spectral asymmetry becomes temperature-dependent. The decrease of the spectral asymmetry at cooling was observed previously by other authors [26]. Unmasking the Fe-O phase highlights the freezing transition near $T_f \approx 230 \text{ K}$ in the PBA phase (wherein the main doublets fade in the right panel of Fig. 3).

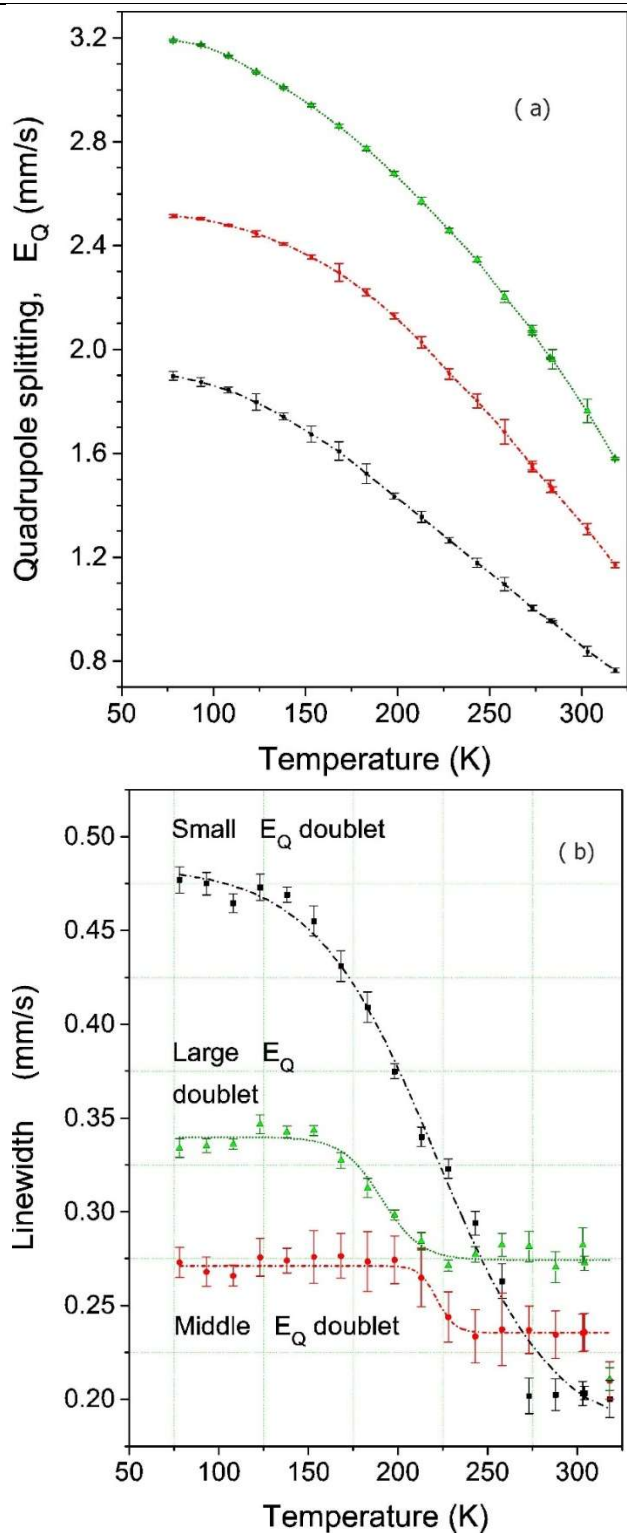


Figure 4. Temperature dependences of the quadrupole splitting (a) and linewidth (b) for three Fe^{2+} quadrupole-split doublets in 2. The lines are guides to the eye.

Temperature dependences of $\Delta E_Q(T)$ and Gaussian linewidths $\Gamma(T)$ are shown in Fig. 4. The inhomogeneous broadening associated with $\Gamma(T)$ reflects the Gaussian distribution of $\Delta E_Q(T)$. The theory explaining the temperature dependences of ΔE_Q was published 50 years ago [27], and in Fe^{2+} the orbital singlet ground state was predicted at that date to produce much larger ΔE_Q (twice, or so) than the orbital doublet ground state.

Temperature dependences of the Gaussian linewidths in Fig. 4 show significant broadening in all three Fe^{2+} doublets that exhibits a step-like variation T_f . Internal doublet with the smallest value of ΔE_Q experiences the strongest broadening; its lines width

increases more than twice. The external doublet increases in width by 30% and the intermediate doublet increases in width by approximately 15%.

Insights into the PBA structure and dynamics have benefited recently, both theoretically and experimentally, from the novelty of molecular dynamics simulations[8] and nuclear inelastic scattering (NIS) studies [25, 28]. The NIS technique enables the access to the Fe-projected phonon DOS, which is related to Mössbauer effect through the Lamb-Mössbauer factor f_{LM} , Eq.(1). One of the first works using the NIS spectroscopy in PBA's [28] was devoted to the vibrational DOS of iron in the inner sphere of the hexacyanometallate complex. In more recent work [25], the vibrations of the Fe^{2+} ion in outer sphere of the complex $[\text{Fe}(\text{py})\{\text{Ni}(\text{CN})_4\}]n\text{H}_2\text{O}$ ($n=2$) were investigated. In this site, the vibrational DOS shows a strong excess of the low-energy excitation. Substituting the DOS $g(E)$ from the Ref. [25] into Eq.(1) we could simulate the Lamb-Mössbauer factor $f_{LM}(T)$ decreasing twice between 77K and 300K (from 0.8 to 0.4). This rapid drop is well consistent with the unmasking effect observed in the plot of the Fe^{3+} area vs. T (Fig.3). Rather small value of $\Delta E_Q=1.18$ mm/s at 310 K, (see Ref. [29], Supporting Information) is similar to ΔE_Q of the inner doublet in Fe-Co PBA. In $[\text{Fe}(\text{py})\{\text{Ni}(\text{CN})_4\}]n\text{H}_2\text{O}$, the water molecules are at the antipodal vertices of the Fe^{2+} coordination polyhedron. This confirms our assignment [30] of the inner doublet to the trans- $\text{Fe}(\text{CN})_4(\text{H}_2\text{O})_2$, as shown in (Fig.1).

The linewidth narrowing of motional nature [31, 32] is a very basic concept, which applies on equal grounds to narrowing of both Γ and ΔE_Q . In crystal fields of high symmetry, the ΔE_Q collapse of motional nature could be a direct consequence of the increased fluctuation rate [33]. Dynamic Jahn-Teller effect underlies typically the fluctuating EFG in a symmetric octahedron, however, in our Fe-Co PBA, the cubic symmetry is broken for majority of the Fe^{2+} sites.

The motional narrowing, related to molecular rotational or librational dynamics in confinement, is sometimes attributed to the appearance of a narrow QS component [34], and in some other instances to the narrowing of Γ [35]. Litterst have observed [35] that the narrowing of Γ can result from an activation of librational motions of a molecule between three conformations with only slight difference of QS. When the fluctuation rate between the conformational states increases sufficiently the narrow doublet with the average QS was observed [35].

In the hydrogen-bonding substructure, the octahedronic cluster of 6 coordinated water molecules interpenetrates with the concentric cube of 8 zeolitic waters [1-3, 8]. As a result the polyhedron of 14 water molecules is formed shaped as tetrakis hexahedron. This is, in other words, the so-called kleeptope of cube having two types of vertexes connected to each other with either 6 or 4 links. On the other hand, when one build up the water clusters using the criteria of energy minimum [36] all the vertexes must be connected with each other by three hydrogen bonds. However, such a «tautomer» of the 14-molecule water cluster does not fit into the PBA void.

In the geometry of the 14-molecule kleeptope of cube, the number of geometric links is in a great excess over the number of possible hydrogen bonds. The confinement within the cube generates the low-gain bonding configurations. The energy

minimum criterion cannot be fulfilled because the cluster is not isolated. As a result the system of hydrogen bonds becomes frustrated. Notably, there appears a number of equivalent configurations of hydrogen bonding within the $(\text{H}_2\text{O})_{14}$ cluster composed of 6 C-waters and 8 Z-waters. These states produce the inhomogeneous broadening Mössbauer doublet. In several works, the water clusters were observed to mediate the electric conduction by the transfer of hydrogen ion, as is evidenced from the increase of conductivity with increasing humidity [37-41]. As the protic conductivity (occurring in Prussian Blues via Grotthuss mechanism [37]) increases with increasing temperature the clusters of $\text{H}_{29}\text{O}_{14}^+$ and/or $\text{H}_{27}\text{O}_{14}^-$ containing the hydronium and/or hydroxide ion become as well populated.

As the temperature increases, the rotational degree of freedom of water molecules unfreezes and the rotations help the diffusive jumps of a proton. The rotations and jumps with increasing temperature become rapid enough to induce the motional narrowing similarly to the previous work [35].

On the other hand, at cooling there occurs the formation of a fixed network of hydrogen bonds which corresponds to the structural arrest in the glass theory. The rate of transitions between the subconformational states drops dramatically and each subconformation acquires its own QS value. The transition from conformon liquid to conformon glass could be analogous to the transition from polaron liquid to polaron glass [42].

The attribution of the slowing down relaxation dynamics to freezing the diffusive and rotational motions of H_2O brings into play the coupling between Z- H_2O and C- H_2O molecules. Since

4. CONCLUSIONS

In Prussian Blues, random occupation of ligand site by CN and water species yields a variety of conformations of these species around a central (Fe) ion. These conformations control the ground state of the central ion whose energy levels are split by the conformational crystal fields. Conformational dynamics addresses the ligand neighbors thermal motion with the displacement amplitudes much larger than their vibrational displacement amplitudes. A composite quasiparticle of both unpaired electron and its conformational surrounding (coined the “conformon”) is a plausible entity to explain the motional narrowing. While the characteristic frequencies of the thermal vibrational excitations are some tens of Terahertz, the conformational excitations are much slower and fall into Megahertz range. Electron flips between

5. REFERENCES

- [1] Buser H., Schwarzenbach D., Petter W., Ludi A., The crystal structure of Prussian blue: $\text{Fe}_4[\text{Fe}(\text{CN})_6]_3 \cdot x\text{H}_2\text{O}$, *Inorganic Chemistry*, 16, 11, 2704-2710, **1977**.
- [2] Herren F., Fischer P., Ludi A., Hälgl W., Neutron diffraction study of Prussian Blue, $\text{Fe}_4[\text{Fe}(\text{CN})_6]_3 \cdot x\text{H}_2\text{O}$. Location of water molecules and long-range magnetic order, *Inorganic Chemistry*, 19, 4, 956-959, **1980**.
- [3] Mullica D., Oliver J., Millig W., Hills F., Ferrous hexacyanocobaltate dodecahydrate, *Inorganic and Nuclear Chemistry Letters*, 15, 9-10, 361-365, **1979**.
- [4] Coronado E. *et al.*, Pressure-tuning of magnetism and linkage isomerism in iron (II) hexacyanochromate, *Journal of the American Chemical Society*, 127, 13, 4580-4581, **2005**.
- [5] Kosaka W., Nomura K., Hashimoto K., Ohkoshi S.-i., Observation of an Fe (II) spin-crossover in a cesium iron

this coupling is weak (ca. 5 kcal/mole) the coupled and decoupled states contribute to the same Mössbauer doublet. Therefore, in PBA, we consider irrelevant an alternative strong-coupling physical picture capable describing the whole set of coexisting Mössbauer doublets as originating from relaxational dynamics [34, 43].

Looking at the behavior of sidebands in ^2H NMR spectra of $\text{Na}_{0.5}\text{Co}_{1.26}\text{Fe}(\text{CN})_6 \cdot x\text{D}_2\text{O}$ the authors of Refs.[44,45] commented on the behavior of C_2 axis of the molecule D_2O . The axis had no fixed orientation above 240 K, owing to the overall rotation of the molecule, however, below 240 K the axis orientation freezes. In this frozen orientation, the flips of D atoms around the axis does not stop down to 200 K, at least. The deuterated water was also explored in the manganese(II) hexacyanochromate(III), without and with partial replacement of 40% of manganese for nickel (in $\text{Mn}_{1.2}\text{Ni}_{0.8}[\text{Cr}(\text{CN})_6]_2 \cdot 12\text{D}_2\text{O}$)[45]. In the latter case, one could not discern in the spectrum between the waters coordinating to manganese and nickel. The water feels the hyperfine field averaged over the solid solution. Both zeolitic and coordination waters freeze below 250 K, and neither Mn nor Ni bind tightly the coordination water above 250 K[45]

There remains in PBA the clear distinction between the discrete Mössbauer doublets owing to large difference of the crystal fields for the cis- and trans- $\text{Fe}(\text{CN})_4(\text{H}_2\text{O})_2$ conformations. In this respect, the PBA stands in contrast to archetypal PB $\text{Fe}_4[\text{Fe}(\text{CN})_6]_3 \cdot 14\text{H}_2\text{O}$, in which owing to vanishing valence contribution to QS [27] the signatures of a variety of the high-spin Fe^{3+} sites merge with each other [30, 46].

crystal field levels couple to the H_2O rotations and H^+ diffusive jumps. These coupled movements are strongly correlated among neighboring cells, rationalized as collective excitations or «conformon» quasiparticles. The hopping time crosses near T_f the lifetime of the excited Mössbauer nucleus ^{57}Fe , so that the crossover becomes observable in ^{57}Fe Mössbauer line widths.

Mössbauer spectra linewidths show the S-like broadening with decreasing temperature in $\text{Fe}_3[\text{Co}(\text{CN})_6]_2 \cdot 12\text{H}_2\text{O}$. The sigmoidal dependences $\Gamma(T)$ are an indication of temperature-distributed structural changes induced by freezing the rotational and conformational dynamics. The onset of a stable network of hydrogen bonds takes place below $T_f = 230$ K.

hexacyanochromate, *Journal of the American Chemical Society*, 127, 24, 8590-8591, **2005**.

[6] Rykov A.I., Wang J., Zhang T., Nomura K., A structural phase transition coupled to the Fe^{3+} spin-state crossover in anhydrous $\text{RbMn}[\text{Fe}(\text{CN})_6]$, *Hyperfine Interactions*, 218, 1-3, 139-143, **2012**.

[7] Rasmussen P.G., Meyers E., An investigation of Prussian blue analogues by Mössbauer spectroscopy and magnetic susceptibility, *Polyhedron*, 3, 2, 183-190, **1984**.

[8] Schulte M., Frank I., Car-Parrinello Simulations of Prussian Blue: Structure, Dynamics, and Electronic Properties, *The Journal of Physical Chemistry C*, 115, 28, 13560-13565, **2011**.

[9] Chernyshov D., Bosak A., Diffuse scattering and correlated disorder in manganese analogue of Prussian blue, *Phase Transitions*, 83, 2, 115-122, **2010**.

[10] Bhatt P., Thakur N., Mukadam M.D., Meena S.S., Yusuf S.M., Evidence for the Existence of Oxygen Clustering and Understanding of

Structural Disorder in Prussian Blue Analogues Molecular Magnet M1. 5 $[\text{Cr}(\text{CN})_6]_z \text{H}_2\text{O}$ (M= Fe and Co): Reverse Monte Carlo Simulation and Neutron Diffraction Study, *The Journal of Physical Chemistry C*, 117, 6, 2676-2687, **2013**.

[11] Golo V., Volkov Y.S., Tunneling of protons and tautomeric transitions in base pairs of DNA, *International Journal of Modern Physics C*, 14, 01, 133-156, **2003**.

[12] Volkenstein M., Electronic-conformational interactions in biopolymers, *Pure and Applied Chemistry*, 51, 4, 801-829, **1979**.

[13] M. V. Volkenstein, The conformon, (in eng), *J Theor Biol*, 34, 1, 193-5, **1972**.

[14] Rykov A.I., Li X., Wang J., Crystal structure refinement of the electron-transfer-active potassium manganese hexacyanoferrates and isomorphous potassium manganese hexacyanocobaltates, *Journal of Solid State Chemistry*, **2015**.

[15] Li X., *et al.*, Excellent photo-Fenton catalysts of Fe-Co Prussian blue analogues and their reaction mechanism study, *Applied Catalysis B: Environmental*, 179, 196-205, **2015**.

[16] Klencsár Z., MossWinn 4.0 Pre Manual, 2012, 11, ed: Nov, **2012**.

[17] Klencsár Z., Transmission integral analysis of Mössbauer spectra displaying hyperfine parameter distributions with arbitrary profile, *MOSSBAUER SPECTROSCOPY IN MATERIALS SCIENCE-2014*, 1622, 30-39, AIP Publishing, **2014**.

[18] Klencsár Z., Kuzmann E., Vértes A., User-friendly software for Mössbauer spectrum analysis, *Journal of Radioanalytical and Nuclear Chemistry*, 210, 1, 105-118, **1996**.

[19] Gütlich P., Link R., Trautwein A., Mössbauer spectroscopy and transition metal chemistry, *Springer Science & Business Media*, **2013**.

[20] Shenoy G., Friedt J., Maletta H., Ruby S., Curve fitting and the transmission integral: warnings and suggestions, in *Mössbauer effect methodology: Springer*, 277-305, **1974**.

[21] Margulies S., Debrunner P., Frauenfelder H., Transmission and line broadening in the Mössbauer effect. II, *Nuclear Instruments and Methods*, 21, 217-231, **1963**.

[22] Williams J.M., Brooks J.S., The thickness dependence of Mössbauer absorption line areas in unpolarized and polarized absorbers, *Nuclear Instruments and Methods*, 128, 2, 363-372, **1975**.

[23] Stieler W., Hillberg M., Litterst F., Böttger C., Hesse J., Numerical evaluation of Mössbauer spectra from thick absorbers, *Nuclear Instruments and Methods in Physics Research Section B: Beam Interactions with Materials and Atoms*, 95, 2, 235-242, **1995**.

[24] Dubiel S., Cieślak J., Alenkina I., Oshtrakh M., Semionkin V., Evaluation of the Debye temperature for iron cores in human liver ferritin and its pharmaceutical analogue, Ferrum Lek, using Mössbauer spectroscopy, *Journal of Inorganic Biochemistry*, 140, 89-93, **2014**.

[25] Félix G., *et al.*, Lattice dynamics in spin-crossover nanoparticles through nuclear inelastic scattering, *Physical Review B*, 91, 2, p. 024422, **2015**.

[26] Reguera E., Yee-Madeira H., Demeshko S., Eckold G., Jimenez-Gallegos J., Nature of the Observed Asymmetry in Mössbauer Spectra of Iron (2+) Hexacyanometallates (III), *Zeitschrift für Physikalische Chemie International journal of research in physical chemistry and chemical physics*, 223, 6, 701-711, **2009**.

[27] Ingalls R., Electric-field gradient tensor in ferrous compounds, *Physical Review*, 133, 3A, A787, **1964**.

[28] Chumakov A.I., Ruffer R., Leupold O., Sergueev I., Insight to dynamics of molecules with nuclear inelastic scattering, *Structural Chemistry*, 14, 1, 109-119, **2003**.

[29] Peng H., *et al.*, Re-Appearance of Cooperativity in Ultra-Small Spin-Crossover $[\text{Fe}(\text{pz})\{\text{Ni}(\text{CN})_4\}]$ Nanoparticles, *Angewandte Chemie*, 126, 41, 11074-11078, **2014**.

[30] Rykov A.I., Wang J., Zhang T., Nomura K., Cs sorption by soluble and insoluble iron hexacyanocobaltates probed by Mössbauer spectroscopy, *Hyperfine Interactions*, 218, 1-3, 53-58, **2013**.

[31] Anderson P.W., A mathematical model for the narrowing of spectral lines by exchange or motion, *Journal of the Physical Society of Japan*, 9, 3, 316-339, **1954**.

[32] Gabuda S., Bound Water. Facts and Hypothesis, *Nauka, Novosibirsk*, 157, **1982**.

[33] Blume M., Tjon J., Mössbauer Spectra in a Fluctuating Environment, *Physical Review*, 165, 2, 446-456, **1968**.

[34] Wellenreuther G., Franz H., Bürck U., Sergueev I., *Rotational dynamics in anisotropic confinement*, *ICAME 2005: Springer*, 141-146, **2007**.

[35] Litterst F.J., Mössbauer studies of crystallization, glass transition and structural relaxation in non-metallic amorphous materials, *Nuclear Instruments and Methods in Physics Research*, 199, 1, 87-97, **1982**.

[36] Farrell J.D., Wales D.J., Clusters of Coarse-Grained Water Molecules, *The Journal of Physical Chemistry A*, 118, 35, 7338-7348, **2014**.

[37] Ohkoshi S.-i., Nakagawa K., Tomono K., Imoto K., Tsunobuchi Y., Tokoro H., High proton conductivity in prussian blue analogues and the interference effect by magnetic ordering, *Journal of the American Chemical Society*, 132, 19, 6620-6621, **2010**.

[38] Xiao C., Chu Z., Ren X.-M., Chen T.-Y., Jin W., Integrated, highly crystalline and water stable coordination framework films on various substrates and water-assisted protonic conductivity, *Chemical Communications*, 51, 37, 7947-7949, **2015**.

[39] Horike S., Umeyama D., Kitagawa S., Ion conductivity and transport by porous coordination polymers and metal-organic frameworks, *Accounts of chemical research*, 46, 11, 2376-2384, **2013**.

[40] Yoon M., Suh K., Natarajan S., Kim K., Proton conduction in metal-organic frameworks and related modularly built porous solids, *Angewandte Chemie International Edition*, 52, 10, 2688-2700, **2013**.

[41] Sadakiyo M., Yamada T., Kitagawa H., Hydrated Proton-Conductive Metal-Organic Frameworks, *ChemPlusChem*, 81, 8, 691-701, **2016**.

[42] Argyriou D., *et al.*, Glass transition in the polaron dynamics of colossal magnetoresistive manganites, *Physical Review Letters*, 89, 3, p. 036401, **2002**.

[43] Gibb T., Anisotropic relaxation of the electric field gradient tensor in the ^{57}Fe Mossbauer spectra of a thiourea-ferrocene clathrate, *Journal of Physics C: Solid State Physics*, 9, 13, p. 2627, **1976**.

[44] S. Takeda, Y. Umehara, H. Hara, and G. Maruta, "Magnetic Local Structures of Prussian-Blue Analogs: Hyperfine Coupling of the Cyanide Ions and the Coordination Water Molecules as Studied by Solid-State ^{13}C and ^2H NMR," *Molecular Crystals and Liquid Crystals*, vol. 379, no. 1, pp. 253-258, **2002**.

[45] H. Ishiyama, G. Maruta, T. Kobayashi, and S. Takeda, "Hyperfine coupling of the cyanide ions and crystal water molecules of three dimensional magnetic polycyanides as studied by solid-state ^{13}C - and ^2H NMR," *Polyhedron*, vol. 22, no. 14, pp. 1981-1987, **2003**.

[46] Greaves T., Cashion J., Site analysis and calculation of the quadrupole splitting of Prussian Blue Mössbauer spectra, *Hyperfine Interactions*, 237, 1, 1-9, **2016**.

6. ACKNOWLEDGEMENTS

This work was supported by the Chinese Academy of Sciences Visiting Professorships for Senior International Scientists (2011T1G15) and the National Natural Science Foundation of China (21476232).

© 2016 by the authors. This article is an open access article distributed under the terms and conditions of the Creative Commons Attribution license (<http://creativecommons.org/licenses/by/4.0/>).